Preoperative Evaluation of Non-Mass-Like Enhancement on Magnetic Resonance Imaging for Measuring Tumor Extent and Affecting Surgical Margin Status in Breast Cancer Patients

Seon Min Park, M.D.*, Eun Young Kim, M.D.*, Yong Lai Park, M.D., Ph.D., Chan Heun Park, M.D., Ph.D.

Department of Surgery, Kangbuk Samsung Hospital, Sungkyunkwan University School of Medicine, Seoul, Korea

Purpose: This study investigated the correlation between non-mass-like enhancement (NME) observed on preoperative breast magnetic resonance imaging (MRI) and the actual pathological size of breast cancer. We further examined the effect of NME on the positive resection margins during partial mastectomy. **Methods:** We retrospectively collected data from breast cancer patients who underwent surgery between January 2018 and September 2020. Patients were divided into two groups based on their MRI findings: NME and no-NME (mass-like lesion only) groups. The medical records, including MRI findings and clinicopathological information of patients, were collected retrospectively, and correlations with pathologic results were analyzed. Propensity score matching was applied to develop comparable cohorts of the NME group and no-NME group. **Results:** This study included a total of 317 patients, with 66 and 251 patients in the NME and no-NME groups, respectively. The mean pathologic size of invasive lesion was significantly smaller than the mean lesion size in the NME group (1.55±1.39 cm vs. 3.45±1.81 cm, $p < 0.001$). The mean pathologic size of ductal carcinoma *in situ* (DCIS) lesions was larger than that in the NME group but without statistical significance (3.91±2.67 cm vs. 3.50±1.79 cm, $p = 0.326$). In the NME group, NME estimated DCIS size to within 1 cm in 20 patients (30.3%) and overestimated invasive lesion size by more than 1 cm in 31 patients (46.9%). NME (vs. no-NME; odds ratio [OR], 2.967; 95% confidence interval [CI], 0.878-10.025) showed a tendency to predict positive resection margins, but this was not statistically significant ($p = 0.080$). **Conclusion:** NME findings on MRI showed a similar extent of DCIS lesions. NME findings on preoperative MRI should be considered an important factor for measuring the extent of tumors, especially in DCIS patients.

Key Words: Breast neoplasms, Carcinoma, Intraductal, Magnetic resonance imaging, Non-infiltrating

INTRODUCTION

Breast cancer is the most common malignancy in South Korean women and is the leading cause of death in Western countries [1]. Magnetic resonance imaging (MRI) is considered the most sensitive method for detecting breast cancer. However, the evaluation of non-mass enhancement (NME) findings in breast MRI is challenging. NME is defined in the Breast Imaging Reporting and Data System (BI-RADS) lexicon of the American College of Radiology (ACR) as an area of enhancement without definite features of a mass [2]. Segmental, lineal, and clumped forms of NME can be associated with both malignant and benign findings. In the fifth edition of the BI-RADS,

the enhancement patterns of NME are categorized as homogeneous, heterogeneous, clumped, and clustered-ring enhancement [3]. Although the reported rate of NME is lower than the rate of mass enhancement on MRI, invasive cancers sometimes present as NME forms on preoperative MRI [4,5]. The differential diagnosis for NME on MRI includes several benign diseases, diseases with high risk, radiation effects, invasive lobular carcinoma, ductal carcinoma *in situ* (DCIS), and invasive carcinoma [6].

The preoperative role of NME in patients with breast cancer varies. Several clinical results have reported the diagnostic performance of NME in detecting primary cancers [7,8]. In this study, we compared the diagnostic performance of NME as detected by preoperative MRI with the aim of determining the accuracy of measuring the tumor extent in breast cancer patients. The second aim of this study was to investigate whether NME is a predictor of positive resection margins in patients with breast cancer undergoing partial mastectomy.

Correspondence: Chan Heun Park, M.D., Ph.D.
Department of Surgery, Kangbuk Samsung Hospital, Sungkyunkwan University School of Medicine, 29 Saemunan-ro, Jongno-gu, Seoul 03181, Korea
Tel: +82-2-2001-1730, Fax: +82-2-2001-1883, E-mail: chanheun1@gmail.com
*These authors contributed equally to this work.

METHODS

Patient selection

This retrospective cohort study was conducted at the Department of Surgery, Kangbuk Samsung Hospital. Patients who underwent breast cancer surgery between January 2018 and September 2020 were included in the study. Patients were selected by reviewing electronic medical charts for invasive breast carcinoma (IBC) and DCIS cases. We excluded patients with breast cancers diagnosed by excisional biopsy, vacuum-assisted breast biopsy, or stereotactic biopsy, or who underwent neoadjuvant chemotherapy. We divided the patients into two groups according to NME findings on MRI: the no-NME and NME groups. NMEs accompanied by a single mass or mass-like lesion were included in the NME group.

Clinical characteristics of patients were analyzed, including age at diagnosis, methods of cancer detection (asymptomatic, symptomatic), size of NME or enhancing mass on MRI, microcalcification on mammography, extensive microcalcifications (microcalcifications involving more than one quadrant of the breast), multifocality of the lesion, and type of surgery (i.e., partial mastectomy, total mastectomy). Missing data were excluded from statistical analysis. This study was approved by the Institutional Review Board (KBSMC2021-05-047).

Interpretation of MRI

MRI was performed using a 3.0-Tesla system (Philips Medical System, Best, Netherlands) equipped with a dedicated 7-channel SENSE breast coil. The following images were acquired after obtaining localized images: T2-weighted (W) turbo spin-echo axial images (repetition time [TR]/echo time [TE], 3,790/100; 332×316 matrix; field of view (FOV), 200×340 mm; slice thickness, 3 mm; gap, 1 mm), T1-W turbo spin-echo axial images (TR/TE, 620/10; 332×332 matrix; FOV, 200×340 mm; slice thickness, 3 mm; gap, 1 mm), and dynamic contrast-enhanced examination using a fat-suppressed T1-W 3D fast field echo sequence (TR/TE, 7.0/3.5; 452×410 matrix; FOV, 340×340 mm; slice thickness, 2 mm; no gap). Finally, delayed axial T1-W spin-echo images (TR/TE, 532/10; 448×378 matrix; FOV, 380×380 mm; slice thickness, 5 mm; gap, 2.5 mm) were acquired to evaluate the axilla using a body coil. Six series of axial dynamic MRI for both breasts were obtained at 0, 1, 2, 3, 5, and 7 minutes after intravenous injection of 1.0 M gadobutrol (Bayer Schering Pharma, Berlin, Germany). MRI reports were interpreted by four breast imaging radiologists following ACR BIRADS [9]. Since data were collected retrospectively, there was no consensus or discordant reports among radiologists.

Histopathological analysis

The pathological characteristics of the tumors were analyzed, including histologic type, size of invasive or *in situ* carcinoma, grade of DCIS, tumor grade (Scarff-Bloom-Richardson grading modified by Elston and Ellis), number of metastatic lymph nodes, presence of *in situ* component, extensive intraductal component (EIC), lymphovascular invasion, estrogen receptor (ER) status, progesterone receptor (PR) status, human epidermal growth factor receptor 2 (HER2) status, subtype, 7th edition of the American Joint Committee on Cancer (AJCC), tumor, node, metastasis (TNM) stage, and status of resection margin after partial mastectomy. The immunohistochemistry-defined subtypes were as follows: luminal A, ER(+) or PR(+), HER2(-); luminal B, ER(+) or PR(+), HER2(+); HER2-enriched, ER(-) and PR(-), HER2(+); and triple-negative, ER(-), PR(-), HER2(-). We further subdivided hormone receptor–positive tumors using the Ki67 labeling index to distinguish luminal B from luminal A tumors ($< 14\%$ for luminal A vs. $\geq 14\%$ for luminal B) [10]. For invasive cancer, a positive resection margin is defined as "ink on tumor" (any invasive cancer or DCIS cells on ink) [11]. For patients with DCIS, a positive resection margin is defined when the tumor cells are ≤ 2 mm from the inked margin [12]. When tumor cells were positive or close to the margin, the tumor was designated for re-excision. When the result was positive or close to the margin after three consecutive margin excisions, partial mastectomy was converted to total mastectomy. Permanent sections were analyzed using paraffin-embedded blocks. All histopathologic analyses were reported by five board-certified pathologists with 10–24 years of experience. Since data were collected retrospectively, there was no consensus or discordant reports among pathologists.

Statistical analysis

Independent two-sample t-tests and Pearson's chi-square tests were used to compare clinicopathological characteristics between patients with NME and those without NME. Paired t-test and McNemar's test were used to evaluate the associations between radiological size and pathological size of cancer.

The extent of NME and mass enhancement on MRI were com-

Seon Min Park, et al. Preoperative Evaluation of NME in Breast Cancer Patients

31

pared to tumor size on histopathology (reference standard) within a range of -1 cm to 1 cm. We set -1 cm to 1 cm as the lower and upper limits for the equivalence test, respectively. If the result was within this boundary, we confirmed it to be equivalent to the histopathological result. Agreements of histopathological tumor size with NME and mass enhancement were evaluated using Bland–Altman plots. Lin's concordance and Pearson correlation coefficients were estimated to assess the agreement among NME, mass enhancement, and histopathologic results. Propensity score matching of 1:1 scheme with a caliper width equal to 0.2 was applied to develop comparable cohorts of patients with NME and no-NME groups. Covariates for matching included age and mass enhancement on MRI.

Univariate and multivariate logistic regressions were used to calculate odds ratios (ORs) with 95% confidence intervals (CIs) for positive margins. A p-value < 0.05 (2-tailed) was considered statistically significant. All statistical analyses were performed using PASW Statistics for Windows (version 18.0; SPSS Inc., Chicago, USA).

RESULTS

Clinicopathological characteristics of the study population

During the study period, 317 patients were diagnosed with either IBC or DCIS. The overall patient group included 251 patients with IBC and 56 patients with DCIS. The mean patient age was 49.97 ± 10.45 years (range, 20–85 years). Among the 317 patients, 66 had NME findings on MRI, and 251 were not associated with NME.

The NME group was more likely to present with microcalcifications on mammography (62.12% vs. 25.11%, $p < 0.001$), extensive microcalcifications on mammogram (10.61% vs. 0.87%, $p = 0.001$), larger size of $in\ situ$ carcinoma (3.90 ± 2.67 cm vs. 1.61 ± 0.87 cm, $p < 0.001$), EIC (43.90% vs. 12.16%, $p < 0.001$), total mastectomy (77.27% vs. 2.79%, $p < 0.001$), and intraoperative resection margin positivity for invasive component only and both DCIS of invasive [30.77% vs. 6.70%, $p = 0.014$, 35.29% vs. 10.78%, $p = 0.011$], respectively. After propensity matching, the NME groups were more likely to present with microcalcifications on mammograms (61.70% vs. 17.78%, $p < 0.001$), larger size of $in\ situ$ carcinoma (4.00 ± 2.87 cm vs. 1.76 ± 0.82 cm, $p < 0.001$), total mastectomy (74.47% vs. 0%, $p < 0.001$), and intraoperative resection margin positivity for the invasive component (33.33% vs. 6.06%, $p = 0.035$). The clinical and pathological features of the patients are shown in Table 1.

Concordance of NME and no−NME with tumor size

The extent of NME and mass enhancement on MRI were compared with the tumor size on histopathology (Table 2). Tumor size was

Table 1. Clinicopathological characteristics of the study population

Characteristic	Total (n = 317) No. (%)	Before propensity score matching			After propensity score matching		
		no-NME group (n = 251) No. (%)	NME group (n = 66) No. (%)	p-value	no-NME group (n = 47) No. (%)	NME group (n = 47) No. (%)	p-value
Age at diagnosis (yr)*	49.97 ± 10.45	50.25 ± 10.64	48.94 ± 9.69	0.366	50.4 ± 12.1	49.81 ± 9.68	0.793
Age at diagnosis (yr)†				0.201			0.678
< 50	170 (53.63)	130 (51.79)	40 (60.61)		25 (53.19)	27 (57.45)	
≥ 50	147 (46.37)	121 (48.21)	26 (39.39)		22 (46.81)	20 (42.55)	
Method of detection†				0.014			0.256
Asymptomatic	157 (50.16)	115 (46.56)	42 (63.64)		23 (50.00)	29 (61.70)	
Symptomatic	156 (49.84)	132 (53.44)	24 (36.36)		23 (50.00)	18 (38.30)	
Extent of NME (cm)*	-	-	3.56 ± 1.87	-			
Mass enhancement on MRI (cm)*	1.57 ± 0.81	1.62 ± 0.82	1.45 ± 0.78	0.191	1.42 ± 0.72	1.45 ± 0.78	0.879
Microcalcifications on mammogram†	99 (33.33)	58 (25.11)	41 (62.12)	< 0.001	8 (17.78)	29 (61.70)	< 0.001
Extensive microcalcifications†	9 (3.03)	2 (0.87)	7 (10.61)	0.001	0	3 (6.38)	0.242
Multifocality†	2 (3.03)	0	2 (3.03)	> 0.999	0	0	> 0.999
Size of invasive carcinoma (cm)*	1.53 ± 1.00	1.53 ± 0.87	1.55 ± 1.38	0.929	1.37 ± 0.76	1.53 ± 1.25	0.495
Size of invasive carcinoma (cm)†				0.222			0.043
≤ 2.0	195 (76.17)	158 (77.83)	37 (69.81)		33 (86.84)	27 (67.50)	
> 2.0	61 (23.83)	45 (22.17)	16 (30.19)		5 (13.16)	13 (32.50)	

(*Continued to the next page*)

Table 1. Continued

Characteristic	Total (n=317) No. (%)	Before propensity score matching			After propensity score matching		
		no-NME group (n=251) No. (%)	NME group (n=66) No. (%)	p-value	no-NME group (n=47) No. (%)	NME group (n=47) No. (%)	p-value
Size of *in situ* carcinoma (cm)*	2.26±1.89	1.61±0.87	3.90±2.67	<0.001	1.76±0.82	4.00±2.87	<0.001
Size of *in situ* carcinoma (cm)[†]				<0.001			<0.001
≤2.0	115 (62.16)	102 (76.69)	13 (25.00)		19 (73.08)	7 (18.92)	
>2.0	70 (37.84)	31 (23.31)	39 (75.00)		7 (26.92)	30 (81.08)	
Histological tumor type[†]				0.259			0.593
DCIS	56 (17.67)	47 (18.73)	13 (19.70)		9 (19.15)	7 (14.89)	
IBC	251 (79.18)	204 (81.27)	53 (80.30)		37 (78.72)	40 (85.11)	
Histological grade[†]				0.428			0.487
Low	81 (33.75)	63 (33.16)	18 (36.00)		16 (42.11)	11 (28.95)	
Intermediate	115 (47.92)	89 (46.84)	26 (52.00)		17 (44.74)	21 (55.26)	
High	44 (18.33)	38 (20.00)	6 (12.00)		5 (13.16)	6 (15.79)	
Grade of DCIS[†]				0.093			0.428
Low	38 (18.91)	33 (22.60)	5 (9.09)		1 (3.70)	3 (7.69)	
Intermediate	130 (64.68)	90 (61.64)	40 (72.73)		17 (62.96)	29 (74.36)	
High	33 (16.42)	23 (15.75)	10 (18.18)		9 (33.33)	7 (17.95)	
Presence of *in situ* component[†]							
EIC[†]	36 (19.05)	18 (12.16)	18 (43.90)	<0.001	6 (20.00)	11 (37.93)	0.128
LVI[†]	39 (15.73)	27 (13.85)	12 (22.64)	0.119	6 (17.14)	10 (25.00)	0.407
ER positivity[†]	265 (83.60)	206 (82.07)	59 (89.39)	0.153	38 (80.85)	41 (87.23)	0.398
PR positivity[†]	232 (73.19)	177 (70.52)	55 (83.33)	0.037	33 (70.21)	37 (78.72)	0.344
HER2 overexpression[†]	57 (18.04)	42 (16.80)	15 (22.73)	0.265	12 (25.53)	10 (21.28)	0.626
Tumor subtypes[†]				0.159			0.53
HR+ HER2-	229 (72.47)	179 (71.60)	50 (75.76)		30 (63.83)	36 (76.6)	
HR+ HER2+	39 (12.34)	29 (11.60)	10 (15.15)		8 (17.02)	6 (12.77)	
HR- HER2+	17 (5.38)	13 (5.20)	4 (6.06)		4 (8.51)	3 (6.38)	
HR- HER2-	31 (9.81)	29 (11.60)	2 (3.03)		5 (10.64)	2 (4.26)	
T stage[†]				0.452			0.261
0 (*in situ*)	60 (18.93)	47 (18.73)	13 (19.70)		9 (19.15)	7 (14.89)	
1	194 (61.20)	156 (62.15)	38 (57.58)		33 (70.21)	28 (59.57)	
2	59 (18.61)	46 (18.33)	13 (19.70)		5 (10.64)	11 (23.40)	
3	4 (1.26)	2 (0.80)	2 (3.03)		0	1 (2.13)	
N stage[†]				0.755			0.381
0	246 (77.6)	192 (76.49)	54 (81.82)		37 (78.72)	39 (82.98)	
1	52 (16.4)	42 (16.73)	10 (15.15)		6 (12.77)	7 (14.89)	
2	13 (4.10)	12 (4.78)	1 (1.52)		3 (6.38)	0	
3	6 (1.89)	5 (1.99)	1 (1.52)		1 (2.13)	1 (2.13)	
AJCC stage[†]				0.891			0.269
0	59 (18.61)	46 (18.33)	13 (19.70)		10 (21.28)	7 (14.89)	
I	154 (48.58)	120 (47.81)	34 (51.52)		26 (55.32)	26 (55.32)	
II	84 (26.50)	68 (27.09)	16 (24.24)		7 (14.89)	13 (27.66)	
III	20 (6.31)	17 (6.77)	3 (4.55)		4 (8.51)	1 (2.13)	
Type of surgery[†]				<0.001			<0.001
Partial mastectomy	259 (81.70)	244 (97.21)	15 (22.73)		47 (100.00)	12 (25.53)	
Total mastectomy	58 (18.30)	7 (2.79)	51 (77.27)		0	35 (74.47)	
Resection margin status (frozen bx)[†]				0.590			0.103
DCIS (-)	28 (66.67)	26 (68.42)	2 (50.00)		4 (57.14)	1 (50.00)	
DCIS (+)	14 (33.33)	12 (31.58)	2 (50.00)		3 (42.86)	1 (50.00)	
Resection margin status (permanent bx)[†]				>0.999			>0.999
DCIS (-)	52 (92.86)	40 (93.02)	12 (92.31)		7 (77.78)	7 (100.00)	
DCIS (+)	4 (7.14)	3 (6.98)	1 (7.69)		2 (22.22)	0	

(*Continued to the next page*)

Seon Min Park, et al. Preoperative Evaluation of NME in Breast Cancer Patients

33

Table 1. Continued

Characteristic	Total (n = 317) No. (%)	Before propensity score matching			After propensity score matching		
		no-NME group (n = 251) No. (%)	NME group (n = 66) No. (%)	p-value	no-NME group (n = 47) No. (%)	NME group (n = 47) No. (%)	p-value
Resection margin status (frozen bx)[†]				0.014			0.035
Invasive (-)	190 (91.79)	181 (93.30)	9 (69.23)		31 (93.94)	8 (66.67)	
Invasive (+)	17 (8.21)	13 (6.70)	4 (30.77)		2 (6.06)	4 (33.33)	
Resection margin status (permanent bx)[†]				0.207			> 0.999
Invasive (-)	253 (96.93)	203 (97.60)	50 (94.34)		37 (97.37)	38 (95.00)	
Invasive (+)	8 (3.07)	5 (2.40)	3 (5.66)		1 (2.63)	2 (5.00)	
Resection margin status in the total population (frozen bx)[†]				0.011			0.103
DCIS or invasive (-)	218 (87.55)	207 (89.22)	11 (64.71)		35 (87.50)	9 (64.29)	
DCIS or invasive (+)	31 (12.45)	25 (10.78)	6 (35.29)		5 (12.50)	5 (35.71)	
Resection margin status in the total population (permanent bx)[†]				0.282			> 0.999
DCIS or invasive (-)	305 (96.21)	243 (96.81)	62 (93.94)		44 (93.62)	45 (95.74)	
DCIS or invasive (+)	12 (3.79)	8 (3.19)	4 (6.06)		3 (6.38)	2 (4.26)	

Data are presented as number of individuals, n (%) or mean ± standard deviation.
NME = non-mass enhancement; MRI = magnetic resonance imaging; DCIS = ductal carcinoma *in situ*; IBC = invasive breast carcinoma; EIC = extensive intraductal component; LVI = lymphovascular invasion; ER = estrogen receptor; PR = progesterone receptor; HR = hormone receptor; HER2 = human epidermal growth factor receptor 2; bx = biopsy; AJCC = American Joint Committee on Cancer.
*Independent two sample t-test; [†]Pearson's chi-square test.

Table 2. Accuracy of tumor size with NME, no-NME, and pathology

Tumor subtype (cm)	Before propensity score matching (n = 66)			After propensity score matching (n = 47)		
	NME, no-NME Pathologic	NME, no-NME	NME, no-NME vs. path p-value	NME, no-NME Pathologic	NME, no-NME	NME, no-NME vs. path p-value
DCIS	3.91 ± 2.67, 1.74 ± 0.85*	3.50 ± 1.79, 1.52 ± 0.84*	0.326, 0.026*	4.00 ± 2.87, 1.76 ± 0.82	3.44 ± 1.78, 1.29 ± 0.72	0.289, 0.050
Invasive	1.55 ± 1.39, 1.55 ± 0.85*	3.45 ± 1.81, 1.66 ± 0.83*	< 0.001, 0.092*	1.53 ± 1.25, 1.37 ± 0.76	3.44 ± 1.84, 1.41 ± 0.75	< 0.001, 0.826
Largest tumor (DCIS or invasive)	3.55 ± 2.56, 1.69 ± 0.85*	3.56 ± 1.87, 1.62 ± 0.82*	0.993, 0.272*	3.49 ± 2.76, 1.64 ± 0.75	3.45 ± 1.85, 1.42 ± 0.72	0.926, 0.137

Data are presented as mean ± standard deviation. NME = non-mass enhancement; DCIS = ductal carcinoma *in situ*.
*n = 251.

measured for each DCIS component, invasive component, and largest tumor size among DCIS or the invasive component in all patients, if available. The radiologic and histopathologic sizes of the cancers were compared to evaluate the concordance between the two values. The mean pathologic size of invasive lesion was significantly smaller than that of the NME group (1.55 ± 1.39 cm vs. 3.45 ± 1.81 cm, $p < 0.001$). The mean pathologic size of DCIS lesions was significantly larger than that of the no-NME group (1.74 ± 0.85 cm vs. 1.52 ± 0.84 cm, $p = 0.026$). The differences between NME, no-NME, and pathological tumor size are shown in Figure 1 using Bland–Altman plots. We established new data using propensity score matching to avoid potential confounding factors. After propensity score matching, 47 patients were allocated to the NME and no-NME groups, and the clinical characteristics between the two groups were similar compared to before propensity score matching (Table 2).

In the NME group (n = 66), NME estimated the DCIS size to within 1 cm in 20 patients (30.3%) and underestimated the tumor size by more than 1 cm in 18 patients (27.3%) (Table 3). NME estimated the invasive lesion size to within 1 cm in 19 patients (28.8%) and overestimated the size by more than 1 cm in 31 patients (46.9%) (Figure 2). In the no-NME group (n = 251), no-NME underestimated the DCIS lesion size to within 1 cm 85 patients (33.8%) (Table 3), while no-NME estimated the invasive lesion size to within 1 cm in 151 patients (60.2%).

Tumor size in the no-NME group showed a poor correlation with DCIS (intraclass coefficient correlation [ICC]: 0.330; 95% CI, 0.148–
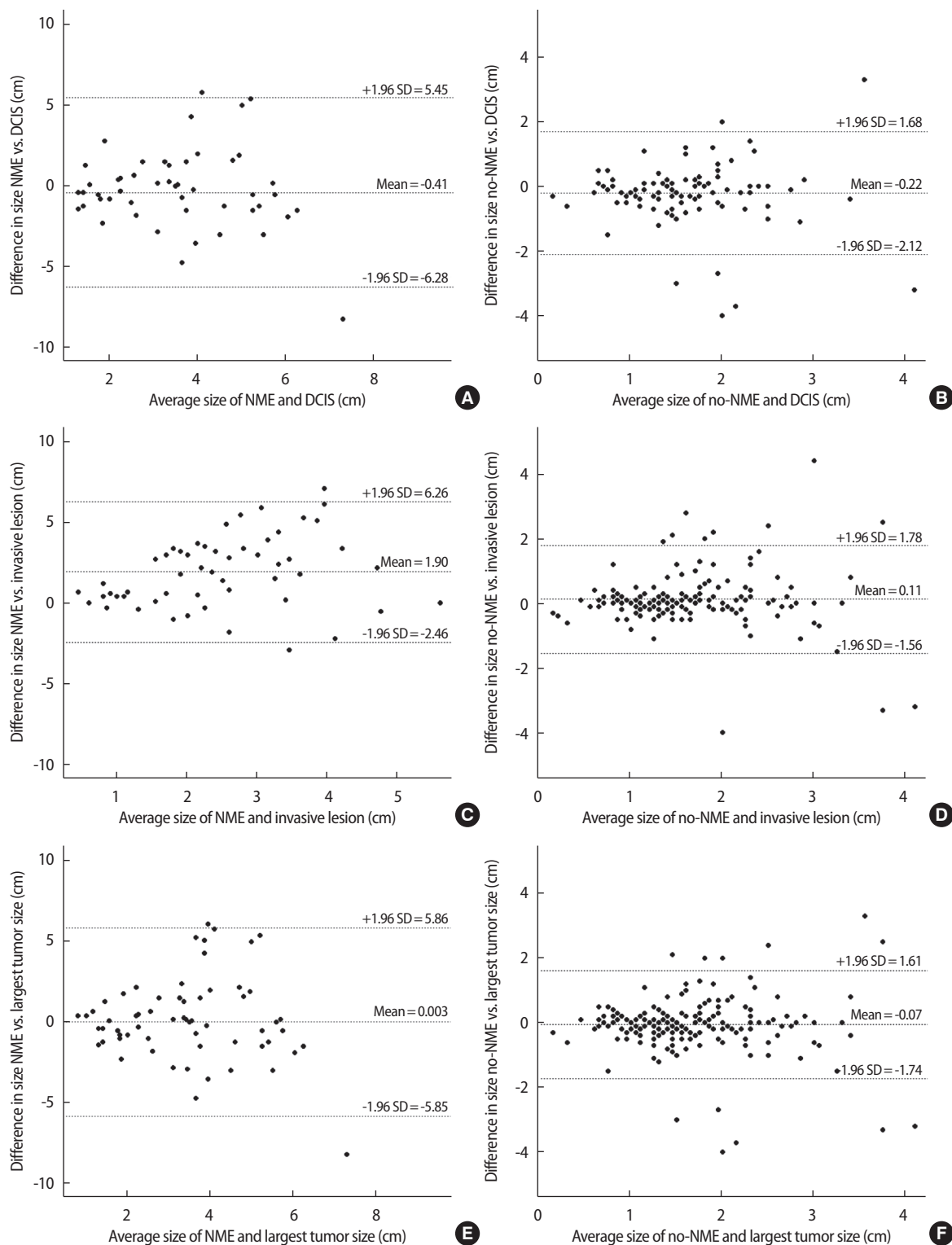
Figure 1. Correlation between DCIS tumor size and NME (A) or no-NME (B); invasive size and NME (C) or no-NME (D); and largest tumor size among DCIS of invasive and NME (E) or no-NME (F) described by Bland–Altman plots. We set -1 cm to 1 cm as the lower and upper limits for the equivalence test, respectively. If the result was within this boundary, we confirmed it to be equivalent to the histopathological result. No systematic bias was found in the differences between histopathological tumor size and NME and no-NME, and variability was consistent across the graph. There is no trend that the difference between methods tends to increase (or decrease) as the average increases. DCIS = ductal carcinoma *in situ*; NME = non-mass enhancement; SD = standard deviation.

Seon Min Park, et al. Preoperative Evaluation of NME in Breast Cancer Patients

35

Table 3. Size estimation in the NME and no-NME groups

Size estimation	NME (n = 66) No. (%)	no-NME (n = 251) No. (%)	*p*-value
DCIS			
vs. Pathology			< 0.001
Overestimates path (> 1 cm)	14 (21.2)	7 (2.8)	
Underestimates path (< -1 cm)	18 (27.3)	8 (3.2)	
Within 1 cm	20 (30.3)	85 (33.8)	
Unknown	14 (21.2)	151 (60.2)	
Invasive			
vs. Pathology			< 0.001
Overestimates path (> 1 cm)	31 (46.9)	16 (6.4)	
Underestimates path (< -1 cm)	3 (4.6)	6 (2.4)	
Within 1 cm	19 (28.8)	151 (60.2)	
Unknown	13 (19.7)	78 (31.0)	
Largest tumor (among DCIS or invasive)			
vs. Pathology			< 0.001
Overestimates path (> 1 cm)	21 (31.8)	12 (4.8)	
Underestimates path (< -1 cm)	19 (28.8)	11 (4.4)	
Within 1 cm	26 (39.4)	176 (70.1)	
Unknown	0	52 (20.7)	

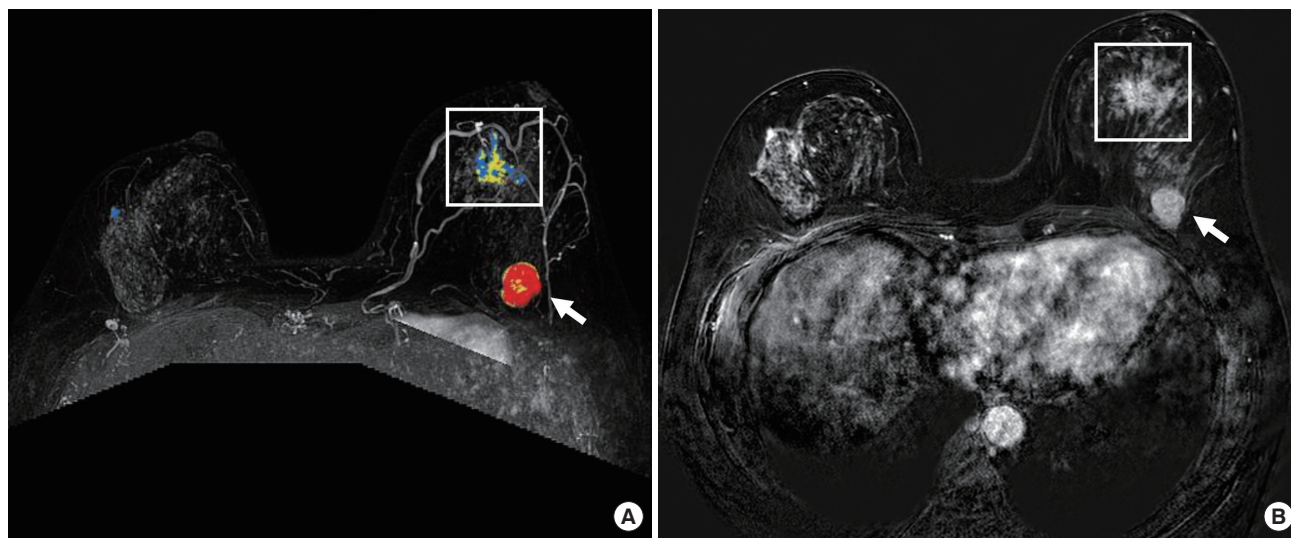NME = non-mass enhancement; DCIS = ductal carcinoma *in situ*.

Figure 2. A 52-year-old woman with invasive carcinoma in the upper center quadrant and DCIS in the upper inner quadrant of the left breast assessed by MRI. A 2.4-cm, round, heterogeneous enhanced mass (arrow) at the 12 o'clock position, 10 cm from the nipple (A, contrast-enhanced dynamic scan; B, subtraction image). A 2.1-cm extent of regional NME (square) at the 10 o'clock position, 3.5 cm from the nipple, was unexpectedly noted on MRI and confirmed as DCIS. DCIS = ductal carcinoma *in situ*; MRI = magnetic resonance imaging; NME = non-mass enhancement.

0.492) and a fair correlation with invasive lesions (ICC: 0.488; 95% CI, 0.366–0.593) (Table 4). Tumor size in the NME group showed a poor correlation with DCIS and invasive lesions.

Univariable and multivariable analyses of factors for a positive surgical margin

In the univariate analysis, DCIS (vs. IBC; OR, 5.371; 95% CI, 2.369–12.179), pTis (vs. T1 OR, 4.968; 95% CI, 2.126–11.61), and AJCC stage 0 (vs. I OR, 4.516; 95% CI, 1.865–10.938) were statistically significant

Table 4. Concordance of NME and no-NME with tumor size

Variable	ICC (95% CI)	Correlation	p-value	Mean difference ± SD	LOA
DCIS					
NME	0.136 (-0.140-0.392)	0.210	0.198	-0.41 ± 3.00	5.87
no-NME	0.330 (0.148-0.492)	0.399	0.001	-0.22 ± 0.97	1.90
Invasive					
NME	0.061 (-0.118-0.212)	-0.143	0.793	1.90 ± 2.22	4.36
no-NME	0.488 (0.366-0.593)	0.491	< 0.001	0.11 ± 0.85	1.67
Largest tumor (among DCIS or invasive)					
NME	0.114 (-0.134-0.347)	0.212	0.196	-2.04 ± 2.85	5.86
no-NME	0.474 (0.359-0.575)	0.475	< 0.001	-0.07 ± 0.86	1.68

NME = non-mass enhancement; ICC = intraclass coefficient correlation; CI = confidence interval; SD = standard deviation; LOA = limit of agreement; DCIS = ductal carcinoma *in situ*.

Table 5. Univariable and multivariable logistic regression of positive resection margin status

Parameter	Univariable		Multivariable	
	OR (95% CI)	p-value	OR (95% CI)	p-value
NME vs. no-NME	2.967 (0.878–10.025)	0.080		
Age at diagnosis (yr)	1.018 (0.980–1.057)	0.356		
Age at diagnosis (yr) (≥ 50 vs. < 50)	1.629 (0.742–3.575)	0.224		
Method of detection				
Symptomatic (lumps) vs. Asymptomatic	0.739 (0.339–1.613)	0.448		
Microcalcifications on mammogram	1.135 (0.474–2.721)	0.776		
Extensive microcalcifications	N/A	-		
Multifocality	N/A	-		
Size of invasive carcinoma (cm) (> 2.0 vs. ≤ 2.0)	0.568 (0.123–2.624)	0.469		
Size of *in situ* carcinoma (cm) (> 2.0 vs. ≤ 2.0)	1.556 (0.600–4.034)	0.364		
Histological tumor type (DCIS vs. Invasive)	5.371 (2.369–12.179)	< 0.001		
Histological grade				
Intermediate vs. Low	3.750 (0.792–17.750)	0.096		
High vs. Low	0.857 (0.075–9.798)	0.901		
Grade of DCIS				
Intermediate vs. Low	3.455 (0.756–15.793)	0.110		
High vs. Low	2.211 (0.337–14.511)	0.409		
Presence of *in situ* component				
EIC (Yes vs. No)	1.450 (0.291–7.223)	0.650		
LVI (Yes vs. No)	0.494 (0.062–3.945)	0.506		
ER positivity (Yes vs. No)	1.429 (0.471–4.334)	0.529		
PR positivity (Yes vs. No)	2.080 (0.760–5.691)	0.154		
HER2 overexpression (Yes vs. No)	1.103 (0.393–3.092)	0.852		
Tumor subtypes				
Luminal B vs. Luminal A	0.529 (0.117–2.383)	0.407		
HER2 vs. Luminal A	2.203 (0.555–8.741)	0.261		
Triple negative vs. Luminal A	0.236 (0.031–1.819)	0.166		
T stage				
Tis vs. T1	4.968 (2.126–11.61)	< 0.001	2.151 (0.055–83.333)	0.683
Tis vs. T2	8.806 (1.86–41.689)	0.006	2.494 (0.038–166.667)	0.670
Tis vs. T3	N/A	-	N/A	-
N stage				
N1 vs. N0	0.337 (0.077–1.482)	0.150		
N2 vs. N0	0.566 (0.07–4.573)	0.594		
N3 vs. N0	N/A	-		
AJCC stage				
0 vs. I	4.516 (1.865–10.938)	0.001	2.151 (0.055–83.333)	0.683
0 vs. II	8.731 (2.33–32.715)	0.001	3.731 (0.069–200)	0.518
0 vs. III	7.226 (0.87–59.992)	0.067	3.003 (0.042–200)	0.614

OR = odds ratio; CI = confidence interval; NME = non-mass enhancement; N/A = not available; DCIS = ductal carcinoma *in situ*; EIC = extensive intraductal component; LVI = lymphovascular invasion; ER = estrogen receptor; PR = progesterone receptor; HER2 = human epidermal growth factor receptor 2; AJCC = American Joint Committee on Cancer.

Seon Min Park, et al. Preoperative Evaluation of NME in Breast Cancer Patients

37

predictors of a positive surgical margin. NME (vs. no-NME; OR, 2.967; 95% CI, 0.878–10.025) also tended to show a positive correlation with positive resection margins, but this was not statistically significant ($p = 0.080$). In the multivariate analysis, there were no predictive factors for positive resection margins (Table 5).

DISCUSSION

Breast MRI is an accurate method for breast cancer detection with an approximate sensitivity of 68.0%–100.0%. MRI also measures the size of the mass forming breast cancer as well as the non-mass form of the tumor. However, the evaluation of non-mass-like lesions on breast MRI is challenging. According to the BI-RADS classification, NME is defined as an area of enhancement without definite features of a mass. NME should be distinguished from the background parenchymal enhancement. Our study found that NME findings on MRI overestimated invasive tumor size, while NME findings on MRI closely estimated the tumor size of the DCIS lesion. In contrast, no-NME findings on MRI closely estimated the extent of invasive lesions, while no-NME findings on MRI underestimated DCIS lesion size.

Many previous studies have shown an association between NME on preoperative breast MRI and positive resection margins. Based on the results of these studies, NME can be considered a predictive factor for positive margins. Park et al. [8] reported that when NMEs were accompanied by a single mass or without a mass-like lesion, the positive resection margin rate during partial mastectomy was more than twice that of cases without NME findings (NME, 36.8% vs. no-NME, 15.4%). Kang et al. [13] also reported that NME with or without mass was an independent predictor of a positive resection margin compared with masses without NME (OR = 7.00, $p < 0.001$). The authors also stated that segmental distribution of NME was strongly associated with a positive resection margin (OR = 11.96, $p = 0.025$). Jang et al. [14] found that NME (OR = 2.96) on preoperative MRI was positively associated with re-excision, and segmental distribution of NME was a predictor of re-excision (OR = 10.53). Our study showed a similar trend. The NME group was more likely to have intraoperative resection margin positivity than the no-NME group (35.3% vs. 10.8%, $p = 0.011$). The NME group was more likely to present with microcalcifications on mammograms (62.1% vs. 25.1%, $p < 0.001$), extensive microcalcifications on mammography (10.6% vs. 0.9%, $p = 0.001$), and

larger size of *in situ* carcinoma (3.90 ± 2.67 cm vs. 1.61 ± 0.87 cm, $p < 0.001$), resulting in more cases of total mastectomy (77.3% vs. 2.8%, $p < 0.001$). The higher resection margin positivity in NME patients could be due to DCIS manifesting as NME. DCIS was accompanied more by the NME pattern than by mass enhancement. Most DCIS cases show segmental or ductal distribution and clustered ring or clumped internal enhancement [15,16].

Several studies have reported that NME findings are often present in histologically diagnosed DCIS cases. In a study conducted by Rosen et al. [17], 59% of pure DCIS cases and 69% of all DCIS lesions presented as NME. A mass-like enhancement was observed in only 14% of DCIS cases. NME, described as segmental distribution, was the most common feature of DCIS on MRI. DCIS, presented as a linear with ductal distribution, was not frequent. For this reason, some investigators have not recommended MRI as a standard diagnostic modality for DCIS [18,19]. However, several studies have investigated and proved the efficacy of MRI in detecting and assessing the size of DCIS [20,21]. The sensitivity of MRI in the detection of DCIS was approximately 77%–96% in those studies. Many other studies have used MRI to predict the extent of DCIS. Especially for pure DCIS, subsegmental, linear, and clumped NME were the most frequent features observed on MRI [22]. Miyashita et al. [23] investigated the correlation between MRI findings and histopathology results in patients diagnosed with DCIS. The authors reported that approximately 80% of the patients had NME findings, and 18% of those patients had invasive lesions on the final histopathology report. Our results revealed that NME lesions were a better factor for estimating the extent of DCIS lesions compared with no-NME lesions. However, there was no statistically significant correlation between NME size and DCIS size.

This study has several limitations. First, the study was performed at a single institution and included a small number of patients in the NME group. Additionally, this study was conducted retrospectively. Second, although the interpretation of preoperative MRI and size measurement of NME lesions was performed according to BI-RADS by experienced radiology specialists, the decision on imaging features might be subjective. Lastly, we could not find differences in tumor extent in NME patients according to immunohistochemistry subtype.

In conclusion, NME findings on MRI showed a similar extent to the DCIS lesion and an increased tendency of margin positivity on intraoperative frozen sections. NME findings on preoperative MRI

should be considered important factors for measuring the extent of tumors, especially in DCIS patients, and as predictors of positive resection margins during partial mastectomy.

CONFLICT OF INTEREST

The authors declare that they have no competing interests.

REFERENCES

1. Heron M. Deaths: leading causes for 2004. Natl Vital Stat Rep 2007;56:1-95.

2. American College of Radiology. BI-RADS: Mammography. Breast imaging reporting and data system: ACR BI-RADS – breast imaging atlas. 4th ed. Reston: American College of Radiology; 2003.

3. Rao AA, Feneis J, Lalonde C, Ojeda-Fournier H. A pictorial review of changes in the BI-RADS fifth edition. Radiographics 2016;36: 623-39.

4. Schnall MD, Blume J, Bluemke DA, DeAngelis GA, DeBruhl N, Harms S, et al. Diagnostic architectural and dynamic features at breast MR imaging: multicenter study. Radiology 2006;238:42-53.

5. Bartella L, Liberman L, Morris EA, Dershaw DD. Nonpalpable mammographically occult invasive breast cancers detected by MRI. Am J Roentgenol 2006;186:865-70.

6. Thomassin-Naggara I, Trop I, Chopier J, David J, Lalonde L, Darai E, et al. Nonmasslike enhancement at breast MR imaging: the added value of mammography and US for lesion categorization. Radiology 2011;261:69-79.

7. Cho YH, Cho KR, Park EK, Seo BK, Woo OH, Cho SB, et al. Significance of additional non-mass enhancement in patients with breast cancer on preoperative 3T dynamic contrast enhanced MRI of the breast. Iran J Radiol 2016;13:e30909.

8. Park MJ, Park MY, Kwon JO, Park KS, Yu YB, Yang JH, et al. Clinical significance of non-mass-like enhancement of preoperative magnetic resonance imaging in breast cancer considering breast-conserving surgery. J Breast Dis 2018;6:20-4.

9. American College of Radiology. ACR BI-RADS atlas : breast imaging reporting and data system. 5th ed. Reston: American College of Radiology; 2013.

10. Cheang MC, Chia SK, Voduc D, Gao D, Leung S, Snider J, et al.

11. Ki67 index, HER2 status, and prognosis of patients with luminal B breast cancer. J Natl Cancer Inst 2009;101:736-50.

11. Moran MS, Schnitt SJ, Giuliano AE, Harris JR, Khan SA, Horton J, et al. Society of Surgical Oncology-American Society for Radiation Oncology consensus guideline on margins for breast-conserving surgery with whole-breast irradiation in stages I and II invasive breast cancer. Int J Radiat Oncol Biol Phys 2014;88:553-64.

12. Morrow M, Van Zee KJ, Solin LJ, Houssami N, Chavez-MacGregor M, Harris JR, et al. Society of Surgical Oncology-American Society for Radiation Oncology-American Society of Clinical Oncology consensus guideline on margins for breast-conserving surgery with whole-breast irradiation in ductal carcinoma in situ. Ann Surg Oncol 2016;23:3801-10.

13. Kang JH, Youk JH, Kim JA, Gweon HM, Eun NL, Ko KH, et al. Identification of preoperative magnetic resonance imaging features associated with positive resection margins in breast cancer: a retrospective study. Korean J Radiol 2018;19:897-904.

14. Jang M, Kim SM, Yun BL, Kim SW, Kang EY, Park SY, et al. Magnetic resonance imaging factors predicting re-excision in breast cancer patients having undergone conserving therapy. J Korean Soc Magn Reson Med 2014;18:133-43.

15. Tozaki M, Fukuda K. High-spatial-resolution MRI of non-masslike breast lesions: interpretation model based on BI-RADS MRI descriptors. Am J Roentgenol 2006;187:330-7.

16. Vag T, Baltzer PA, Dietzel M, Benndorf M, Gajda M, Camara O, et al. Kinetic characteristics of ductal carcinoma in situ (DCIS) in dynamic breast MRI using computer-assisted analysis. Acta Radiol 2010;51:955-61.

17. Rosen EL, Smith-Foley SA, DeMartini WB, Eby PR, Peacock S, Lehman CD. BI-RADS MRI enhancement characteristics of ductal carcinoma in situ. Breast J 2007;13:545-50.

18. Daniel BL, Yen YF, Glover GH, Ikeda DM, Birdwell RL, Sawyer-Glover AM, et al. Breast disease: dynamic spiral MR imaging. Radiology 1998;209:499-509.

19. Boetes C, Strijk SP, Holland R, Barentsz JO, Van Der Sluis RF, Ruijs JH. False-negative MR imaging of malignant breast tumors. Eur Radiol 1997;7:1231-4.

20. Marcotte-Bloch C, Balu-Maestro C, Chamorey E, Ettore F, Raoust I, Flipo B, et al. MRI for the size assessment of pure ductal carcinoma in situ (DCIS): a prospective study of 33 patients. Eur J Radiol 2011;

Seon Min Park, et al. Preoperative Evaluation of NME in Breast Cancer Patients

39

77:462-7.

21. Lee J, Jung JH, Kim WW, Park CS, Lee RK, Kim HJ, et al. Efficacy of breast MRI for surgical decision in patients with breast cancer: ductal carcinoma in situ versus invasive ductal carcinoma. BMC Cancer 2020;20:934.

22. Jansen SA, Newstead GM, Abe H, Shimauchi A, Schmidt RA, Karczmar GS. Pure ductal carcinoma in situ: kinetic and morphologic MR characteristics compared with mammographic appearance and nuclear grade. Radiology 2007;245:684-91.

23. Miyashita M, Amano G, Ishida T, Tamaki K, Uchimura F, Ono T, et al. The clinical significance of breast MRI in the management of ductal carcinoma in situ diagnosed on needle biopsy. Jpn J Clin Oncol 2013;43:654-63.